Mean ISM abundances (black points)

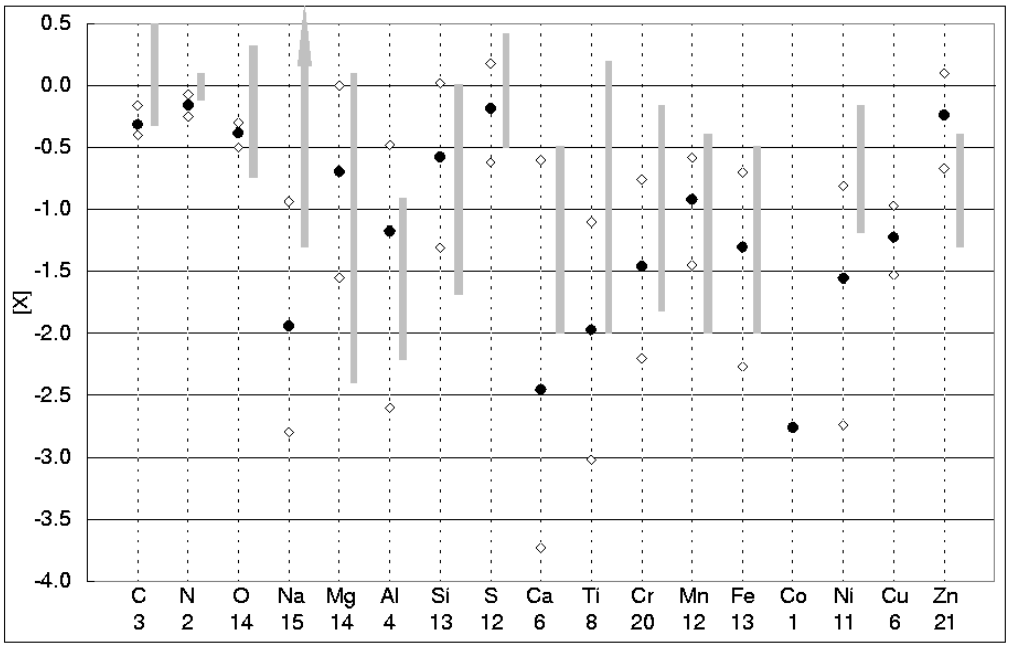

Lodders (2003)

EQUILIBRIUM CONDENSATION TEMPERATURES FOR A SOLAR-SYSTEM COMPOSITION GAS

Element (1)	T_C (K) (2)	Initial Phase {Dissolving Species} (3)	50% T_C (K) (4)	Major Phase(s) or Host(s) (5)
H	182	H_2O ice	...	...
He	<3	He ice	...	...
Li		{Li_4SiO_4, Li_2SiO_3}	1142	Forsterite + enstatite
Be		{$BeCa_2Si_2O_7$}	1452	Melilite
B		{$CaB_2Si_2O_8$}	908	Feldspar
C	78	$CH_4 \cdot 7H_2O$	40	$CH_4 \cdot 7H_2O + CH_4$ ice
N	131	$NH_3 \cdot H_2O$	123	$NH_3 \cdot H_2O$
O	182	Water ice[a]	180	rock + water ice
F	739	$Ca_5[PO_4]_3F$	734	F apatite
Ne	9.3	Ne ice	9.1	Ne ice
Na		{$NaAlSi_3O_8$}	958	Feldspar
Mg	1397	Spinel		
	1354	Forsterite[b]	1336	Forsterite
Al	1677	Al_2O_3	1653	Hibonite
Si	1529	Gehlenite		
	1354	Forsterite[b]	1310	Forsterite + enstatite
P	1248	Fe_3P	1229	Schreibersite
S	704	FeS	664	Troilite
Cl	954	$Na_4[Al_3Si_3O_{12}]Cl$	948	Sodalite
Ar	48	$Ar \cdot 6H_2O$	47	$Ar \cdot 6H_2O$
K		{$KAlSi_3O_8$}	1006	Feldspar
Ca	1659	$CaAl_{12}O_{19}$	1517	Hibonite + gehlenite
Sc		{Sc_2O_3}	1659	Hibonite
Ti	1593	$CaTiO_3$	1582	Titanate
V		{VO, V_2O_3}	1429	Titanate
Cr		{Cr}	1296	Fe alloy
Mn		{Mn_2SiO_4, $MnSiO_3$}	1158	Forsterite + enstatite
Fe	1357[c]	Fe metal[c]	1334	Fe alloy
Co		{Co}	1352	Fe alloy
Ni		{Ni}	1353	Fe alloy
Cu		{Cu}	1037	Fe alloy
Zn		{Zn_2SiO_4, $ZnSiO_3$}	726	Forsterite + enstatite

FITZPATRICK AND MASSA (1988)

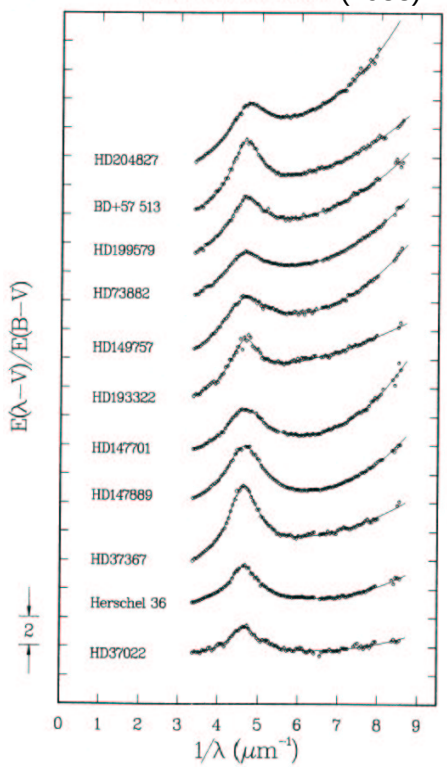

Extinction efficiency for spherical grains from Mie theory

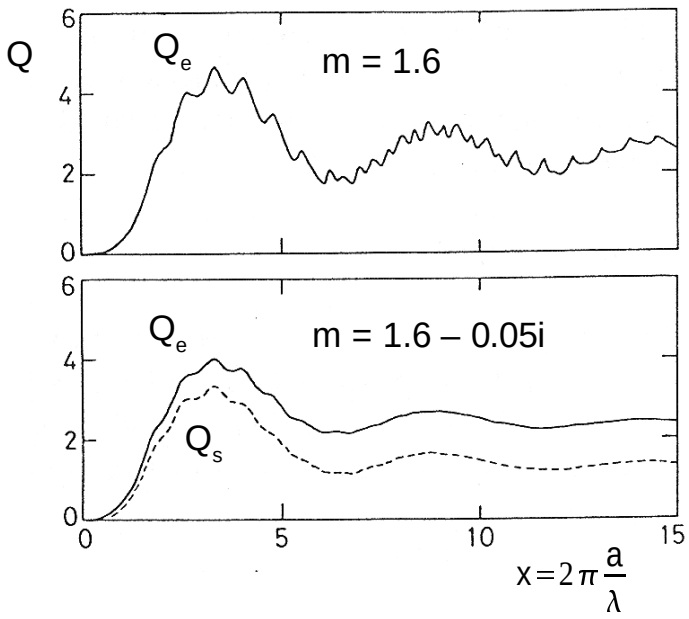

Refractive index:
$m = m_R + m_I\, i$
m_R ... Scattering
m_I ... Absorption

$Q_e = Q_a + Q_s$

Extinction cross-section
$\sigma_e = \pi\, a^2\, Q_e$

a ... grain radius
λ ... wavelength

Whittet D.C.B, 1992, *Dust in the Galactic Environment*

Average observed extinction and dust model of Draine & Lee (1984)

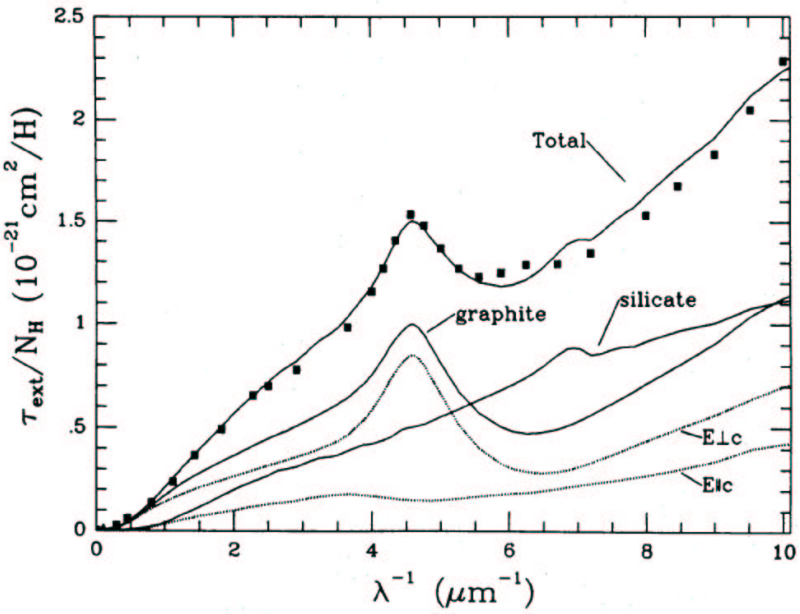

Size distribution:

$$dn_i = A_i\, n_H\, a^{-3.5} da$$

$$[a,\ a + da]$$

$$a_{min} < a < a_{max}$$

$a_{min} \approx 0.005\ \mu m$

$a_{max} \approx 0.25\ \mu m$

MARTIN AND WHITTET (1990)

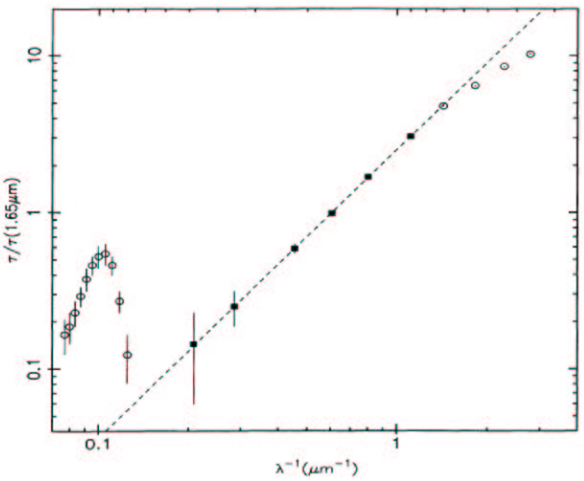

FIG. 1.—Absolute extinction curve for diffuse dust with 10 μm silicate feature adapted from Rieke and Lebofsky (1985). Dashed curve is the power-law fit with slope $\alpha = 1.84$.

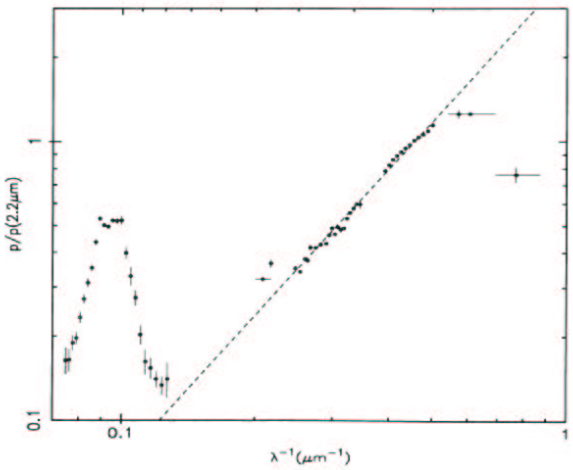

FIG. 4.—Polarization for the molecular cloud source GL 2591. A 10 μm silicate feature is present (Aitken *et al.* 1988). The continuum power law shown has slope $\beta = 1.75$.

L270 D. Lutz et al.: SWS observations of the Galactic center

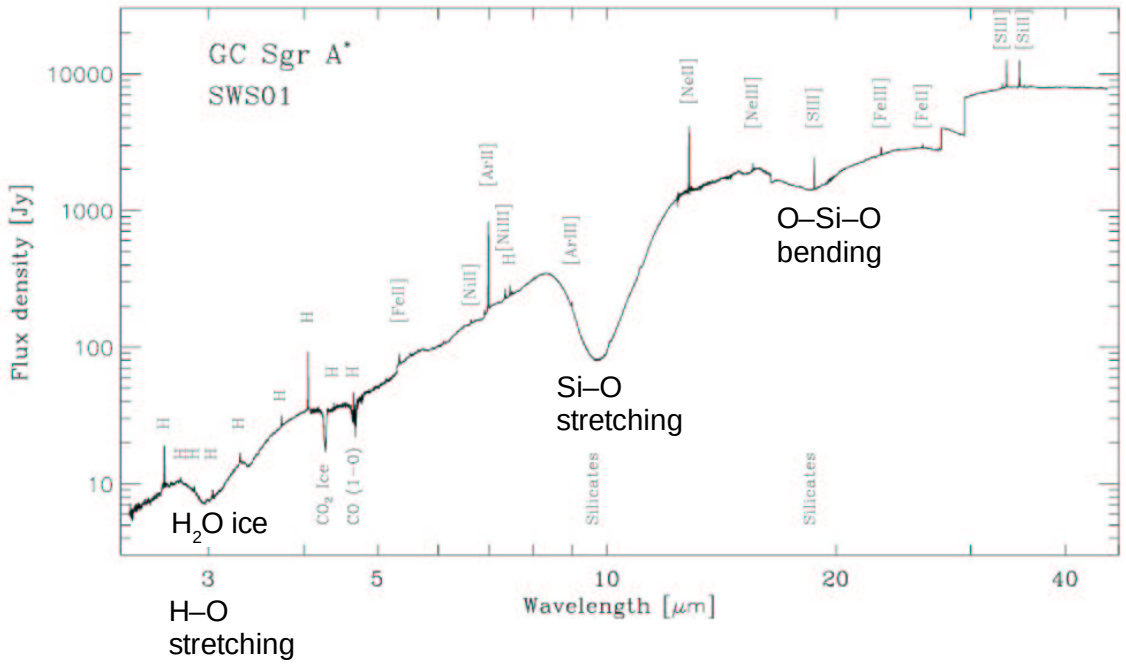

Silicate emission in Orion (Cesarsky et al. 2000)

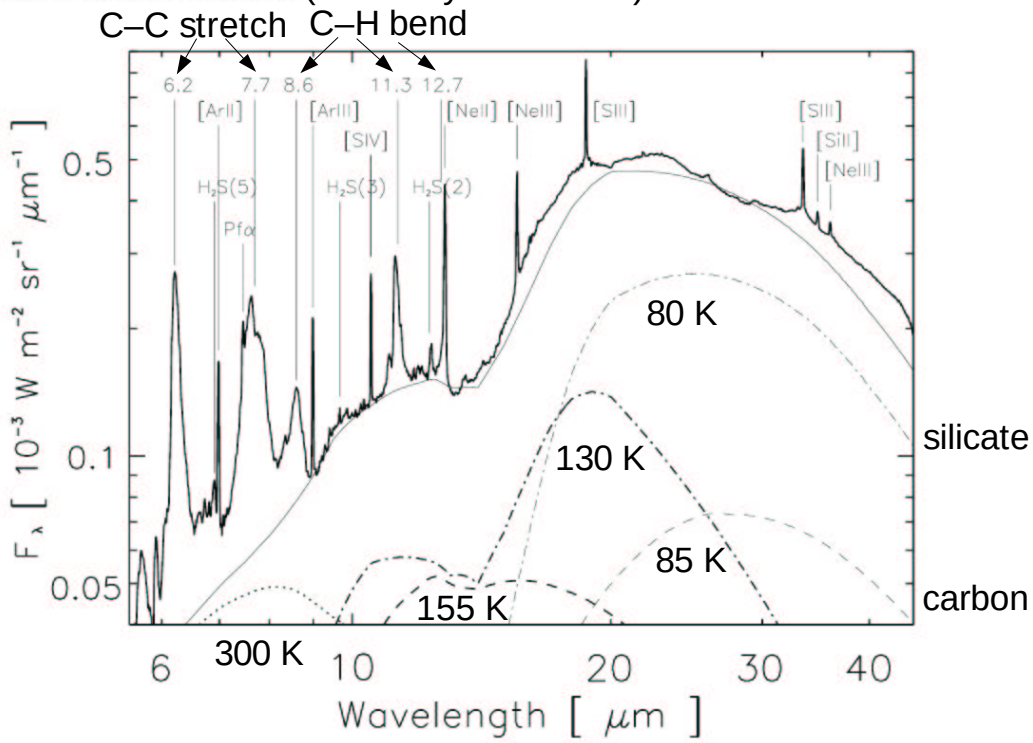

Photoluminescence spectra from Si crystals (Ledoux et al. 1998)

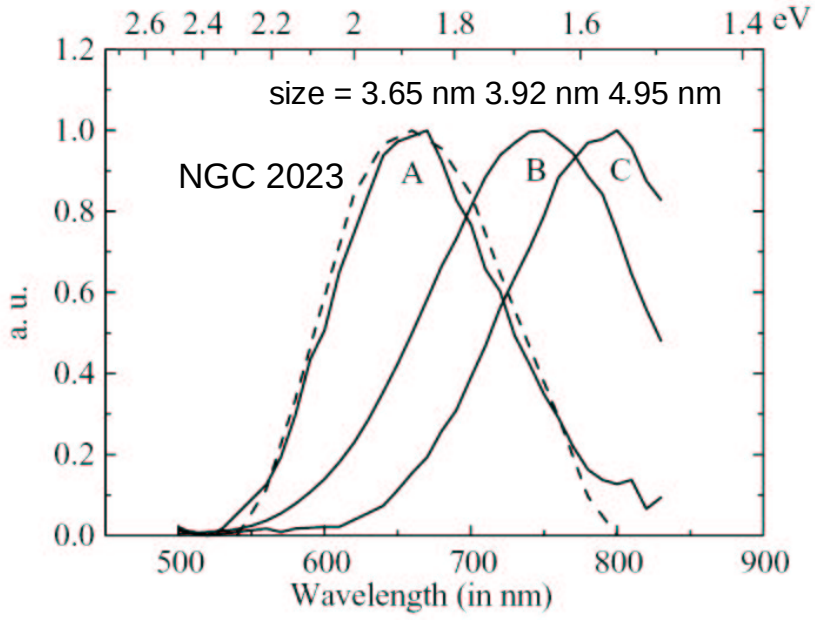

Witt et al. (1998)

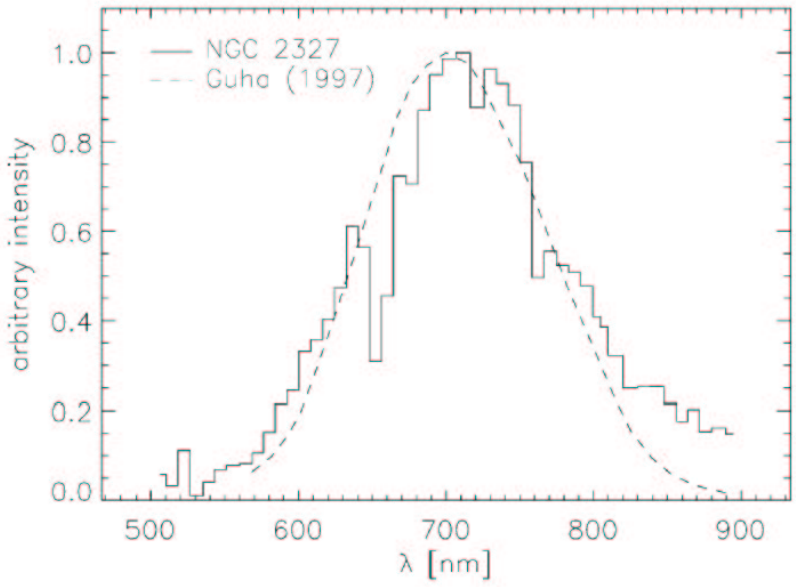

FIG. 1.—The observed ERE spectrum of NGC 2327 (Witt 1988) is plotted along with the photoluminescence of film *B* at room temperature from Guha (1997). Film *B* has a porosity of 70% that corresponds to a particle size of 4 nm.

Time dependence of grain temperature (Draine 2003)

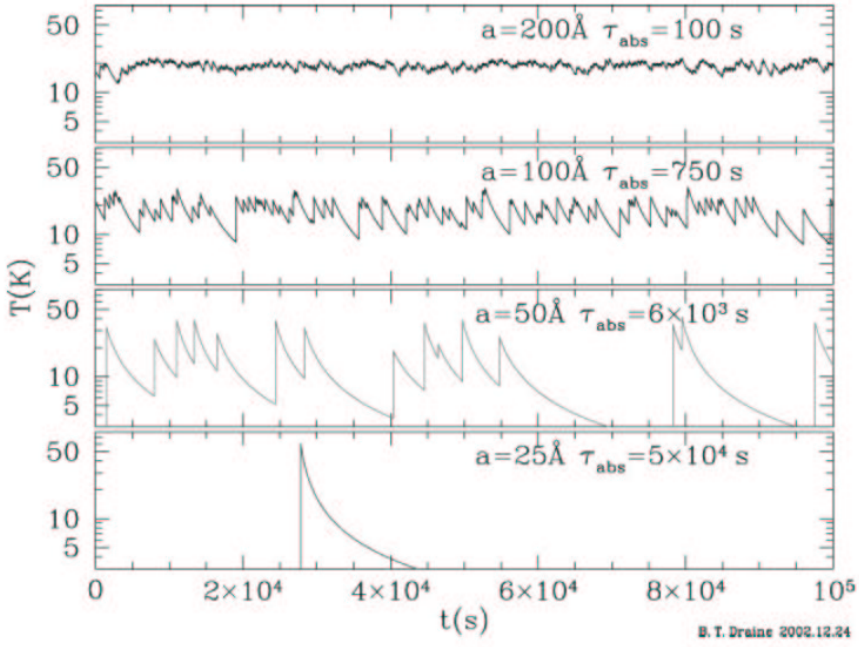

Figure 13 A day in the life of four carbonaceous grains, heated by the local interstellar radiation field. τ_{abs} is the mean time between photon absorptions